NASA TECHNICAL NOTE

NASA TN D-5515

THE EFFECT OF OBJECT MOTION IN FRAUNHOFER HOLOGRAPHY WITH APPLICATION TO VELOCITY MEASUREMENTS

by William P. Dotson, Jr.

Manned Spacecraft Center
Houston, Texas

NATIONAL AERONAUTICS AND SPACE ADMINISTRATION • WASHINGTON, D. C. • NOVEMBER 1969

1. REPORT NO.	2. GOVERNMENT ACCESSION NO.	3. RECIPIENT'S CATALOG NO.
NASA TN D-5515		

4. TITLE AND SUBTITLE	5. REPORT DATE
THE EFFECT OF OBJECT MOTION IN FRAUNHOFER HOLOGRAPHY WITH APPLICATION TO VELOCITY MEASUREMENTS	November 1969
	6. PERFORMING ORGANIZATION CODE

7. AUTHOR(S)	8. PERFORMING ORGANIZATION REPORT NO.
William P. Dotson, Jr., MSC	S-220

9. PERFORMING ORGANIZATION NAME AND ADDRESS	10. WORK UNIT NO.
Manned Spacecraft Center Houston, Texas 77058	039-00-00-00-72
	11. CONTRACT OR GRANT NO.

12. SPONSORING AGENCY NAME AND ADDRESS	13. REPORT TYPE AND PERIOD COVERED
National Aeronautics and Space Administration Washington, D. C. 20546	Technical Note
	14. SPONSORING AGENCY CODE

15. SUPPLEMENTARY NOTES

16. ABSTRACT

The in-line Fraunhofer hologram is analyzed with the assumption that the object moves a significant distance during the observation time. An equation is derived which predicts the effect that object motion has upon the recorded fringe pattern. An analysis of the fringe pattern recorded on the film consequently yields the total motion of the object during the observation time. It is also possible to reconstruct the resultant hologram so that the path the object traveled during the exposure time is reproduced. This knowledge, coupled with the exposure time, yields the desired measurement of the object velocity.

17. KEY WORDS (SUPPLIED BY AUTHOR)	18. DISTRIBUTION STATEMENT
* Laser Velocimeter * Moving Object Holography * Fraunhofer Holography * Holographic Velocimetry	Unclassified - Unlimited

19. SECURITY CLASSIFICATION (THIS REPORT)	20. SECURITY CLASSIFICATION (THIS PAGE)	21. NO. OF PAGES	22. PRICE
Unclassified	Unclassified	24	$3.00 *

*For sale by the Clearinghouse for Federal Scientific and Technical Information
Springfield, Virginia 22151

THE EFFECT OF OBJECT MOTION IN FRAUNHOFER HOLOGRAPHY WITH APPLICATION TO VELOCITY MEASUREMENTS

By William P. Dotson, Jr.*
Manned Spacecraft Center

SUMMARY

This study is concerned with the development of a theory to describe the effect that object velocity has upon the recorded fringe pattern in Fraunhofer holography. The conclusion is that, under the conditions described, objects may move as much as 10 times their mean diameter during the observation time. This motion produces fringes in the hologram which are descriptive of the motion.

INTRODUCTION

A theoretical analysis is made of the time dependence of the intensity of the total field at a recording $\xi\eta$-plane due to the interference of a constant-background field with the field diffracted by a moving object. This equation is then integrated over the observation time in order to find the total energy distribution function in the $\xi\eta$-plane.

This study expands present Fraunhofer holography theory to include moving objects, and the expanded theory is reduced to the usual result found in the literature when the object is stationary. An experiment was designed to test the theory of this study and was performed successfully.

The author extends his appreciation to G. P. Bonner, N. K. Shankar, and C. W. Wells of the Science and Applications Directorate, NASA Manned Spacecraft Center, Houston, Texas, for their assistance in performing the laboratory experiments.

SYMBOLS

A aperture dimensions

$C = -ik/2\pi z_1$

*Captain, U.S. Air Force, assigned to NASA Manned Spacecraft Center.

D	object transmission function
d	object dimension
I	intensity of an electromagnetic field
$i = \sqrt{-1}$	
J	energy density function
K	amplitude of the reference electromagnetic field
$k = 2\pi/\lambda$	
L	lens term, a quadratic phase factor
R	length of the loci of points an object will cover during τ
r	distance from a point on the object to a point in the $\xi\eta$-plane
s_x	x-coordinate of the displacement of the x'y'-plane from the xy-plane
s_y	y-coordinate of the displacement of the x'y'-plane from the xy-plane
T	transform of the object field
t	time
V	transform of the object velocity
v	object velocity
x, y	input plane coordinates
x', y'	coordinate system lying in the xy-plane but centered on the object
z	optical axis
z_1	distance from the xy-plane to the $\xi\eta$-plane
ζ	lead, linear translation per revolution
λ	wavelength of the coherent light source
ξ, η	recording plane coordinates
τ	observation or exposure time
χ	inclination factor for a Huygens radiator

ψ total electromagnetic field amplitude

ψ_o part of ψ due to the object field

ψ_r part of ψ due to the reference field

Superscript:

* conjugate

THE FRAUNHOFER DIFFRACTION THEORY FOR MOVING OBJECTS

Reference is made in the following analysis to figure 1 in which three coordinate systems are indicated. The coordinate system centered on the object is used only once to indicate a translation of the object center. Thereafter, only the input xy-plane and the recording $\xi\eta$-plane will be used.

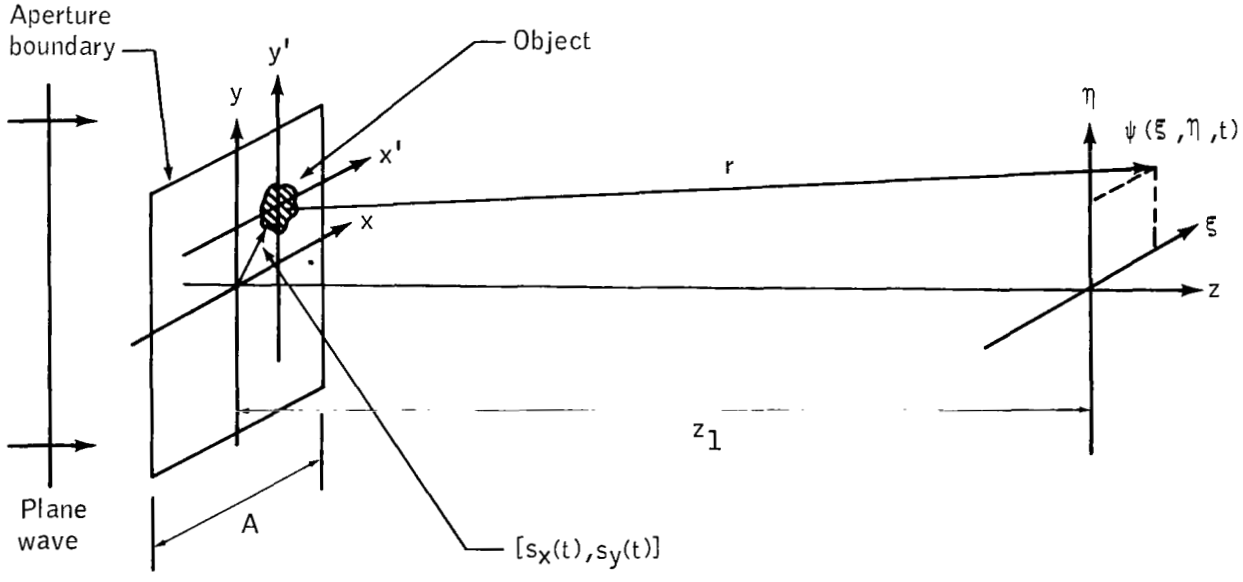

Figure 1. - Geometry for finding $\psi(\xi, \eta, t)$.

Boundary Conditions

By looking into the xy-plane from the right, an observer sees a hole (due to the object) in the field of constant amplitude and phase. If an amplitude of K and a phase of $0°$ is assumed for the plane wave impinging on the xy-plane, the boundary conditions of the problem are

$$\psi(x, y) = \begin{cases} KD(x', y'), & \text{over the object cross section} \\ = K, & \text{elsewhere in the aperture} \end{cases} \tag{1}$$

where $D(x', y')$ represents the object transmission function.

Since the field is linear, superposition may be used. This enables the solution of two relatively simple problems, as opposed to a single more complex problem. Therefore, $\psi(x, y)$ is represented as the sum of the reference field and the object field, as follows.

$$\psi(x, y) = \psi_r(x, y) + \text{object field} \tag{2}$$

where the reference field

$$\psi_r(x, y) = K \tag{3}$$

over the entire aperture.

To express the object field properly, the following definitions are required. If the object is centered at the origin of the xy-plane, then

$$\text{object field} \cdot \equiv_D \psi_o(x, y) \tag{4}$$

If the same object is centered at the origin of the x'y'-plane, which has a displacement of (s_x, s_y) from the xy-plane, then

$$\text{object field} \cdot \equiv_D \psi_o(x', y') = \psi_o\left(x-s_x, y-s_y\right) \tag{5}$$

Therefore

$$\psi(x, y) = \psi_r(x, y) + \psi_o\left(x-s_x, y-s_y\right) \tag{6}$$

where

$$\psi_o\left(x-s_x, y-s_y\right) = \begin{cases} -K(1 - D), & \text{over the object cross section} \\ = 0, & \text{elsewhere in the aperture} \end{cases} \tag{7}$$

Under these conditions, the field in the $\xi\eta$-plane (ref. 1) due to $\psi_r(x, y)$ is, to a close approximation

$$\psi_r(\xi, \eta) = K \exp\left(-ikz_1\right) \tag{8}$$

provided that

$$\frac{A^2}{\lambda} >> z_1 \tag{9}$$

Fresnel Integral

Under ordinary circumstances, a derivation of the diffracted field at the $\xi\eta$-plane due to the object field in the xy-plane is pointless because the problem has already been solved. However, the treatment of this problem is fundamental to later developments because the objective of this study is to find the field at the $\xi\eta$-plane with the object in motion; hence, the object will occupy many positions during the observation time. The symmetry of the usual problem has been removed by placing the object off the optical axis, as shown in figure 1.

The physics of the problem are understood by considering the object field as a summation of a number of point sources and by applying the Huygens principle (ref. 2). Therefore, the differential field at the $\xi\eta$-plane is

$$d\psi_o(\xi, \eta) = \chi\psi_o\left(x-s_x, y-s_y\right) dx\, dy\left(\frac{1}{r}\right)\exp(-ikr) \tag{10}$$

where χ is an inclination factor for the Huygens radiator. The total field is then

$$\psi_o(\xi, \eta) = \int \chi \psi_o\left(x-s_x, y-s_y\right)\left(\frac{1}{r}\right)\exp(-ikr)dx\, dy \tag{11}$$

where the integral is a surface integral with limits set by the physical limits of the object geometry.

To evaluate the integral, r must be found in terms of the coordinates.

$$r = \left[z_1^2 + (\xi - x)^2 + (\eta - y)^2\right]^{1/2} \tag{12}$$

By the binomial series expansion, if

$$z_1^2 \geq 10\left[(\xi - x)^2_{max} + (\eta - y)^2_{max}\right] \tag{13}$$

then, to a close approximation

$$r = z_1 \left\{1 + \frac{1}{2}\left[\frac{(\xi - x)^2 + (\eta - y)^2}{z_1^2}\right]\right\} \tag{14}$$

or

$$r = z_1 + \frac{\xi^2 + \eta^2}{2z_1} + \frac{x^2 + y^2}{2z_1} - \frac{\xi x + \eta y}{z_1} \tag{15}$$

Substituting equation (15) into equation (11) and realizing that amplitude variations in $1/r$ will be small gives the Fresnel integral solution to the problem.

$$\psi_o(\xi, \eta) = \left(\frac{\chi}{z_1}\right)\exp\left(-ikz_1\right)\exp\left[\frac{-ik\left(\xi^2 + \eta^2\right)}{2z_1}\right]$$
$$\int \psi_o\left(x-s_x, y-s_y\right)\exp\left[\frac{-ik\left(x^2 + y^2\right)}{2z_1}\right]\exp\left[\frac{ik(\xi x + \eta y)}{z_1}\right]dx\, dy \tag{16}$$

Far-Field Conditions

Equation (16) is the integral for Fresnel diffraction. The equation for Fraunhofer diffraction is derived from equation (16) by placing constraints on the term $\exp\left[-ik\left(x^2 + y^2\right)/2z_1\right]$ which appears inside the integral. If constraints are placed on this term such that it remains constant (or nearly constant), the term may be taken out of the integral. The magnitude of this term is always unity, but its phase varies according to the limits of integration. These limits are set by the object geometry if the object is stationary. In the example considered by this study, the limits of integration are set by the largest dimension of the loci of points occupied by the object during the observation time. The definition is then

$$R_D \equiv \text{largest dimension of the loci of points occupied by the object during the observation time} \tag{17}$$

If the magnitude of R is such that the phase change of the term $\exp\left[-ik\left(x^2 + y^2\right)/2z_1\right]$ is equal to or less than $\pi/2$, the phase term should remain sufficently constant to be removed from the integral. The requirement is

$$\frac{kR^2}{2z_1} \leq \frac{\pi}{2} \tag{18}$$

or

$$z_1 \geq \frac{2R^2}{\lambda} \tag{19}$$

In the usual case of stationary objects, the argument R is replaced by the object dimension d, and the result is

$$z_1 \geq \frac{2d^2}{\lambda} \tag{20}$$

Equation (20) is often reduced to (ref. 3)

$$z_1 \geq \frac{d^2}{\lambda} \tag{21}$$

since experiment results indicate that equation (21) is adequate to assure the relative constancy of the phase term.

Recalling the definition of R, it is clear that equations (19) and (20) may be combined to yield

$$z_1 \geq \left(\frac{R}{d}\right)^2 2\left(\frac{d}{\lambda}\right)^2 \tag{22}$$

Experiment results indicate that equation (22) may be reduced to

$$z_1 \geq \left(\frac{R}{d}\right)^2 \left(\frac{d^2}{\lambda}\right) \tag{23}$$

Equations (22) and (23) then reduce to equations (20) and (21), respectively, for the case of stationary objects because, by definition, R becomes equal to d.

Fraunhofer Integral

Provided equation (23) is satisfied, the Fresnel integral (eq. (16)) reduces to

$$\psi_o(\xi, \eta) = \left(\frac{\chi}{z_1}\right) \exp\left(-ikz_1\right) \exp\left[\frac{-ik\left(\xi^2 + \eta^2\right)}{2z_1}\right] \exp\left[\frac{-ik\left(x_{av}^2 + y_{av}^2\right)}{2z_1}\right]$$
$$\int \psi_o\left(x-s_x, y-s_y\right) \exp\left[\frac{ik(\xi x + \eta y)}{z_1}\right] dx\, dy \tag{24}$$

where x_{av} and y_{av} indicate the average positions of the object center during the observation time.

If it is imagined that the coordinate systems of figure 1 are set up so that x_{av} and y_{av} are both equal to zero, then

$$\psi_o(\xi, \eta) = \left(\frac{\chi}{z_1}\right) \exp\left(-ikz_1\right) \exp\left[\frac{-ik\left(\xi^2 + \eta^2\right)}{2z_1}\right]$$
$$\int \psi_o\left(x-s_x, y-s_y\right) \exp\left[\frac{ik(\xi x + \eta y)}{z_1}\right] dx\, dy \tag{25}$$

Note that the integral of equation (25) is a two-dimensional Fourier transform. By using the Fourier translation theorem (ref. 4), if

$$f(x) \rightarrow F\left(\frac{k\xi}{z_1}\right) \tag{26}$$

then

$$f(x-x') \rightarrow F\left(\frac{k\xi}{z_1}\right)\exp\left(\frac{ik\xi x'}{z_1}\right) \tag{27}$$

By applying equation (27) in two-dimensional form to equation (25)

$$\psi_o(\xi,\eta) = \left(\frac{\chi}{z_1}\right)\exp(-ikz_1)\exp\left[\frac{-ik(\xi^2+\eta^2)}{2z_1}\right]\exp\left[\frac{ik(\xi s_x + \eta s_y)}{z_1}\right]$$
$$\int \psi_o(x,y)\exp\left[\frac{ik(\xi x + \eta y)}{z_1}\right]dx\,dy \tag{28}$$

The implication of equation (28) is that the object, for integration purposes, may be treated as if it were always centered at the origin of the xy-plane. Hence, the object transform is a function of the object geometry only. The displacement of the object from the origin of the xy-plane is always performed by the modifying term $\exp\left[ik(\xi s_x + \eta s_y)/z_1\right]$ which appears outside the integral. The separation of this displacement term from the surface integration over the object is an important result. This result will be used in the following section to generate a distribution function proportional to the displacement of the object, as a function of time, during the observation period.

Energy Distribution Function Over the Observation Time in the $\xi\eta$-Plane

In this section, time dependence will be placed on s_x and s_y appearing in equation (28). The total field in the $\xi\eta$-plane will be found at any instant of time by summing equations (8) and (28). For convenience, the following definitions are made.

1. The ratio χ/z_1 may be evaluated from a Green's function solution to the problem depicted in figure 1. The result is (ref. 1)

$$\frac{\chi}{z_1} \simeq \frac{-ik}{2\pi z_1} \cdot \equiv_D C \tag{29}$$

2. The lens term

$$L \cdot \equiv_D \exp\left[\frac{-ik\left(\xi^2 + \eta^2\right)}{2z_1}\right] \tag{30}$$

3. The transform

$$T \cdot \equiv_D \int \psi_o(x, y) \exp\left[\frac{ik(\xi x + \eta y)}{z_1}\right] dx\, dy \tag{31}$$

The total field at the $\xi\eta$-plane at any instant of time is due to the summation of the reference field of equation (8) and the object field of equation (28).

$$\psi(\xi, \eta, t) = K \exp\left(-ikz_1\right) + \exp\left(-ikz_1\right) CLT \exp\left\{\frac{ik\left[\xi s_x(t) + \eta s_y(t)\right]}{z_1}\right\} \tag{32}$$

Upon removing the common phase term $\exp\left(-ikz_1\right)$ and setting K equal to 1

$$\psi(\xi, \eta, t) = 1 + CLT \exp\left\{\frac{ik\left[\xi s_x(t) + \eta s_y(t)\right]}{z_1}\right\} \tag{33}$$

The instantaneous intensity at the $\xi\eta$-plane is

$$I(\xi, \eta, t) = \psi(\xi, \eta, t)\psi^*(\xi, \eta, t) \tag{34}$$

where * means conjugate.

Forming the product indicated by equation (34)

$$I(\xi,\eta,t) = 1 + |CT|^2 + CLT \exp\left\{\frac{ik\left[\xi s_x(t) + \eta s_y(t)\right]}{z_1}\right\}$$

$$+ C^*L^*T^* \exp\left\{\frac{-ik\left[\xi s_x(t) + \eta s_y(t)\right]}{z_1}\right\} \tag{35}$$

The following should be noted concerning equation (35).

1. With zero displacement and no motion of the object, equation (35) reduces to the usual result found in the literature (refs. 1, 3, and 5) for the problem depicted in figure 1.

2. If an attempt is made to form a hologram, using the setup shown in figure 1 as an experiment base, the film does not record the intensity given by equation (35). The film actually records the total energy received; that is, the transmittance of the hologram (ref. 6) is proportional to

$$J(\xi,\eta,\tau) = \int_{-\tau/2}^{\tau/2} I(\xi,\eta,t)dt \tag{36}$$

where τ is the observation or exposure time. In equation (36), the film is assumed to be a linear recorder.

Upon performing the operation indicated by equation (36), the total energy distribution function in the $\xi\eta$-plane is

$$J(\xi,\eta,\tau) = \tau + |CT|^2\tau + CLT\int_{-\tau/2}^{\tau/2} \exp\left\{\frac{ik\left[\xi s_x(t) + \eta s_y(t)\right]}{z_1}\right\}dt$$

$$+ C^*L^*T^*\int_{-\tau/2}^{\tau/2} \exp\left\{\frac{-ik\left[\xi s_x(t) + \eta s_y(t)\right]}{z_1}\right\}dt \tag{37}$$

INTERPRETATION OF EQUATION (37)

Equation (37) consists of four terms. The first two terms form a background field which is essentially constant. On this background field, the third and fourth terms

impress variations proportional to the object geometry and the displacement of the object as a function of time. Attention may be restricted to the third term because the fourth term is simply the conjugate of the third term. In the third term, only the last two factors, T and the integral, need to be considered because C is a constant and L is a lens term which controls the formation distance of the hologram of equation (37).

Distribution Functions

The two factors of interest appear in product form in the third term of equation (37). These two factors are

$$T \cdot \equiv_{D} \int \psi_{o}(x, y) \exp\left[\frac{ik(\xi x + \eta y)}{z_1}\right] dx\, dy \tag{31}$$

and

$$V \cdot \equiv_{D} \int_{-\tau/2}^{\tau/2} \exp\left\{\frac{ik\left[\xi s_x(t) + \eta s_y(t)\right]}{z_1}\right\} dt \tag{38}$$

Both T and V are distribution functions. If $s_x(t)$ and $s_y(t)$ are linear, both T and V are Fourier transforms. For illustrative purposes, the situation in which both T and V are Fourier transforms is considered.

The Fourier transform variables in both cases (T and V) are ξ/z_1 and η/z_1. Equation (31) transforms a function of x and y, the object field in the xy-plane, to a function of ξ/z_1 and η/z_1. Equation (38) transforms a function of time, the displacement of the object in the xy-plane, to a function of ξ/z_1 and η/z_1. Because these two functions (eqs. (31) and (38)) appear in product form in the $\xi\eta$-plane, either equation may be forced (by proper control of system parameters in a measurement experiment) to be dominant with respect to the other. The dominant equation will be the one which produces a distribution function with a smaller physical area of interest than the other equation produces.

Dominant Function

To understand how either distribution function (eq. (31) or (38)) may be forced to be dominant with respect to the other function, figure 2 must be considered. Figure 2

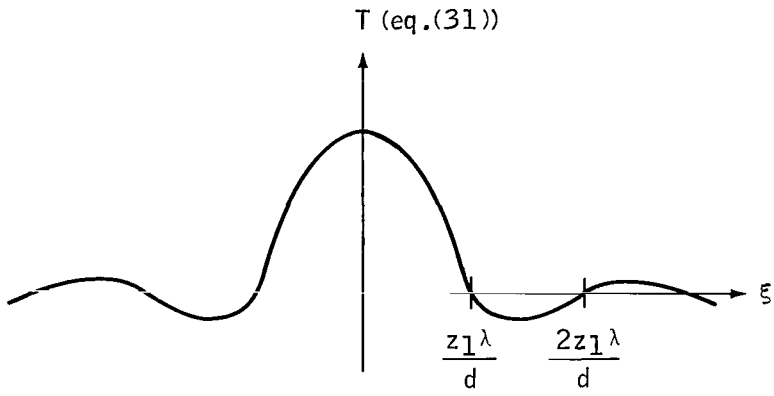

(a) Distribution of T.

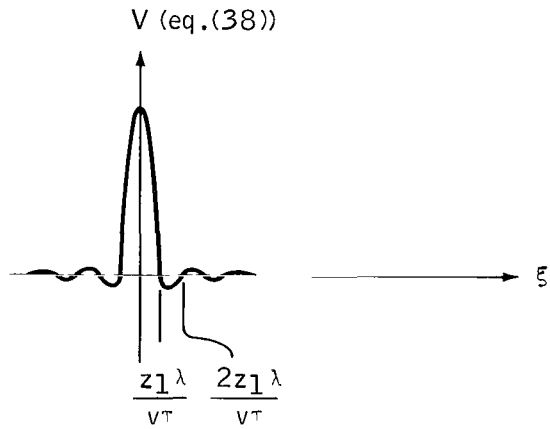

(b) Distribution of V.

Figure 2. - Distribution functions of T and V.

shows a cross section for T when the object is a square with dimension d and a cross section for V when the displacement of the object, as a function of time, is given by vt.

$$s_x(t) = vt \tag{39}$$

$$s_y(t) = 0 \tag{40}$$

The evaluation of equations (31) and (38) is as follows. If it is assumed that the object is opaque, then by equation (7) with $K = 1$

$$\psi_o(x, y) = -1 \tag{41}$$

and

$$T = \int_{-d/2}^{d/2} \int_{-d/2}^{d/2} (-1)\exp\left[\frac{ik(\xi x + \eta y)}{z_1}\right] dx\, dy \tag{42}$$

which is of the form

$$\left(\frac{\sin \frac{k\xi d}{2z_1}}{\frac{k\xi d}{2z_1}}\right)\left(\frac{\sin \frac{k\eta d}{2z_1}}{\frac{k\eta d}{2z_1}}\right)$$

The cross section in the ξ-direction is plotted for T in figure 2.

$$V = \int_{-\tau/2}^{\tau/2} \exp\left[\frac{ik(\xi vt + \eta 0)}{z_1}\right] dt \tag{43}$$

which is of the form

$$\left(\frac{\sin \frac{k\xi v\tau}{2z_1}}{\frac{k\xi v\tau}{2z_1}}\right)$$

The cross section in the ξ-direction is plotted for V in figure 2. In figure 2, the cross section is shown for $v\tau >> d$. In this situation, the object transform T, which multiplies the transform of the displacement function of the object V, acts as a constant of unity with respect to V. Hence, V is said to be dominant and, therefore, is recorded by the film in preference to T. On reconstruction of a hologram which was recorded in the situation where $v\tau > d$ and which satisfies the condition of equation (23), the image which appears in the reconstruction plane will be of the path traveled by the

object during the observation time τ. However, if $v\tau < d$, then T becomes the dominant function. This condition is the usual situation encountered in the literature (refs. 1, 3, 4, and 5).

Limiting Conditions

Equation (37) is valid only if equation (23) is satisfied. It has been shown in reference 1 that a further condition which must be satisfied in Fraunhofer holography is

$$z_1 \leq \frac{100d^2}{\lambda} \tag{44}$$

Equation (44) must be satisfied in order to achieve a usable signal-to-noise ratio in the recorded fringe pattern. From consideration of equations (23) and (44) and of figure 2

$$v\tau \leq 10d \tag{45}$$

Consideration of equation (45) and figure 2 yields the conditions under which fringes which are proportional to the object velocity may be recorded in the hologram.

$$d < v\tau \leq 10d \tag{46}$$

and since $v\tau \rightarrow R$, equation (23) becomes

$$z_1 \geq \left(\frac{v\tau}{d}\right)^2\left(\frac{d^2}{\lambda}\right) \tag{47}$$

The limiting condition given by equation (45) is probably of the greatest interest. From the inequality $v \leq 10d/\tau$, the highest velocities measurable appear to be subject to the fundamental limitations of the pulse width and coherence length of the light source (laser) used. The inequality appears to indicate that no upper limit to measurable velocities exists if τ is required to approach zero. However, during the observation time, enough energy must still be supplied to expose the film; this requirement implies use of high-power pulsed lasers. Under this condition, the observation time τ becomes synonymous with the pulse width of the laser. The coherence length decreases as the pulse width decreases, and ultimately, the coherence length of the light source is too small to be used for holography.

Reasonable expectations of the state of the art in pulsed-laser technology with controllable pulse widths would indicate pulse widths of approximately 1 microsecond. Then if, for example, 1-millimeter objects were measured for their velocities, the highest measurable velocity would be 10 km/sec. Use of objects as large as 1 millimeter would, however, require a special lens arrangement to keep the experiment within the confines of the laboratory walls, as indicated by equation (47).

Applications

The technique presented in this study could be used for a wide range of velocity measurements of particles in the micron range. With a suitable lens arrangement, perhaps larger particles could be measured. Flow studies could be made on fluids seeded with micron-size particles. The technique would perhaps be most useful in situations where present measurement techniques fail; for example, in the measurement of dispersion rates of contaminants around a spacecraft.

Read-Out Device

The experiment results of this study are given in terms of microdensitometer traces. However, because equation (37) is descriptive of the fringes recorded on the film, there is no reason why the resultant hologram cannot be reconstructed to produce the image of the path traveled by the object during the observation time. Velocity measurement is an almost direct measurement because the path length divided by the exposure time yields the velocity. This technique for measuring velocity eliminates the need to know z_1 and λ. These two parameters, in a plane-wave construction and reconstruction, control only the distance from the hologram to the image plane; the image plane can be located visually by seeking the sharpest focus.

EXPERIMENT RESULTS

During the development of the theory discussed in this report, two questions concerning the validity of the two assumptions made in the study were raised.

1. The Fourier translation theorem is well known and is accepted for displacements which do not vary with time. However, is the theorem valid for displacements which vary with time? It was tacitly assumed in the transition from equation (25) to equation (26) and from equation (26) to equation (27) that the theorem was valid.

2. Is the film a sufficiently linear recorder to allow the transition from equation (35) to equation (36) and from equation (36) to equation (37)?

To provide the most convincing answer to the validity questions, an experiment on a one-dimensional object moving with a constant velocity was designed. The devised experiment was simple for two reasons. First, the experiment was sufficient to resolve the previously discussed questions; second, the experiment provided an understanding of the effect of T and V (eqs. (31) and (38)) upon each other.

The Experiment Arrangement

The experiment arrangement used is shown in figure 3. The equipment used was as follows.

1. The light source was a continuous-wave helium-neon laser which operated at a 6328-angstrom wavelength.

2. The object was an opaque wire, approximately 109 microns in diameter, which moved into the page (fig. 3) with a variable velocity v.

3. The object was transported by means of a linear actuator with a lead of 0.1 inch per revolution.

4. The linear actuator was driven by a motor shaft which could be varied from a speed of 0 to 5000 rpm.

5. A 35-millimeter camera was used in the recording $\xi\eta$-plane. The exposure time was 1/125 of a second, and the film was type SO-233.

6. The formation distance z_1 was 94 centimeters.

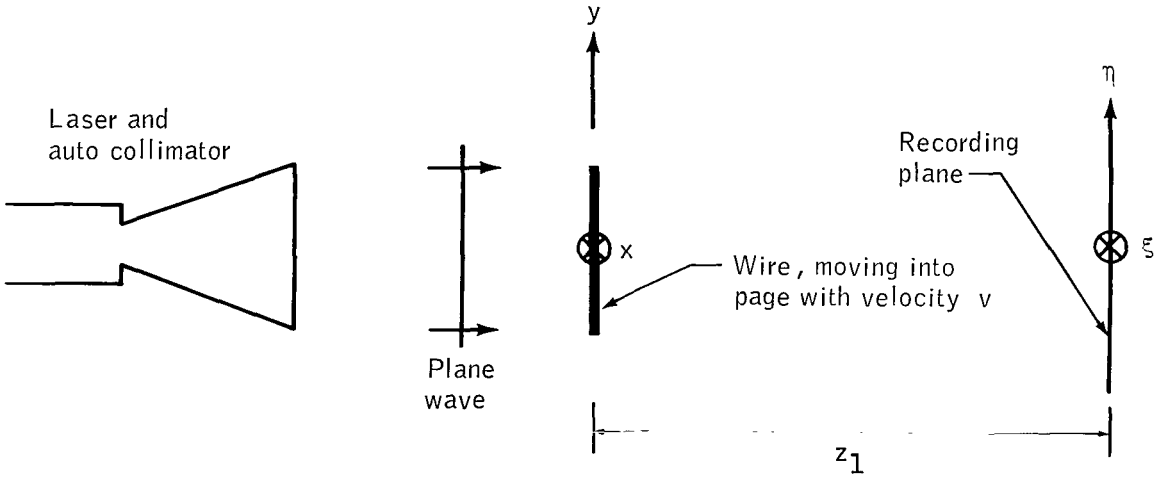

Figure 3. - Experimental arrangement.

Several experiments were performed with all system parameters, except the object velocity, kept constant. Each experiment was performed twice, once at maximum laser intensity and once at lower laser intensity. Table I shows the experiments performed and the controls on each experiment.

TABLE I. - EXPERIMENTS PERFORMED AND CONTROLS

Laser intensity	Experiment no.	z_1, cm	d, microns	τ, sec	Linear actuator lead ζ, cm/rev	Linear actuator shaft, rpm	Object velocity, cm/sec	$v\tau$, microns	Remarks
High	1a	94	109	1/125	0.254	0	0	0	$v\tau < d$
Low	1b	94	109	1/125	.254	0	0	0	$v\tau < d$
High	2a	94	109	1/125	0.254	642	2.72	218	$v\tau > d$
Low	2b	94	109	1/125	.254	642	2.72	218	$v\tau > d$
High	3a	94	109	1/125	0.254	964	4.09	327	$v\tau > d$
Low	3b	94	109	1/125	.254	964	4.09	327	$v\tau > d$

Comparison of Theory and Experiment

Figures 4 to 9 graph the experiment results. A check of experiment measurements versus theoretically predicted measurements of the distance from the center of T or V, depending on which was dominant (fig. 2 and eqs. (31) and (38)), to the first zero crossing was made for each experiment. A comparison of these measurements is presented in table II. The measurement intervals on figures 4 to 9 indicate the experimentally determined positions of the first zeros and the centers of each experiment figure.

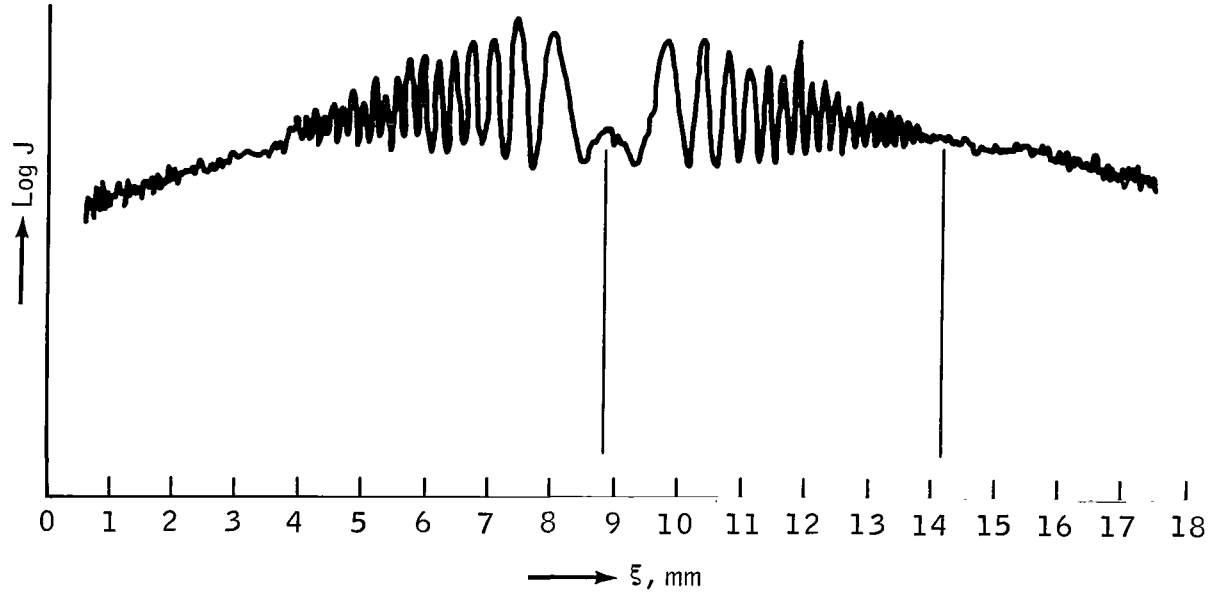

Figure 4. - Microdensitometer trace of experiment 1a.

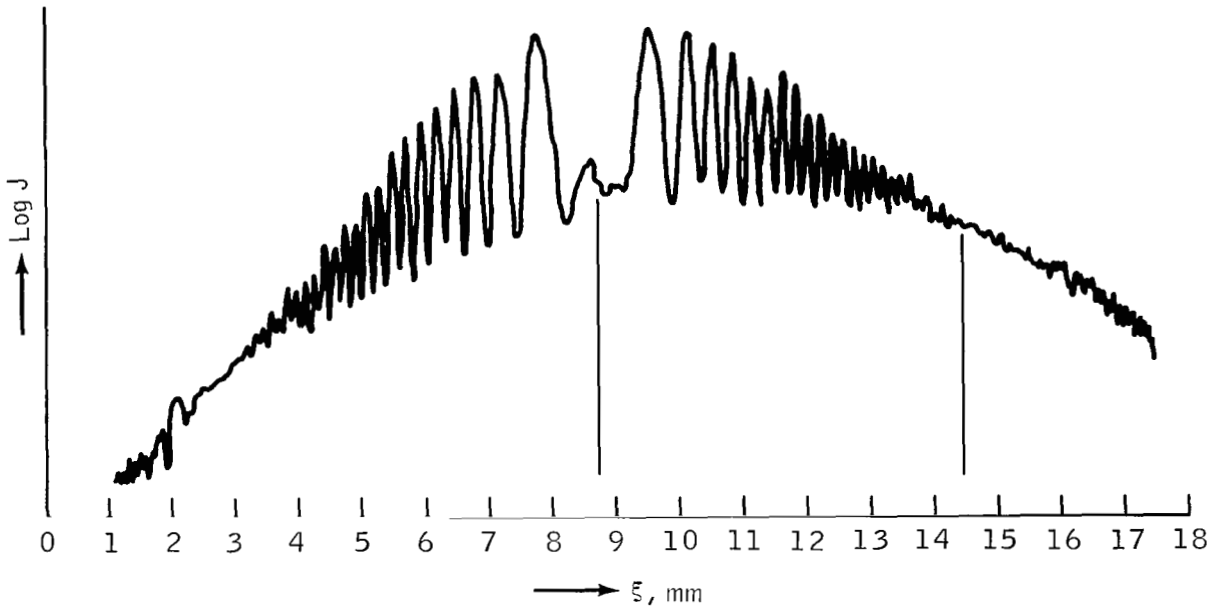

Figure 5. - Microdensitometer trace of experiment 1b.

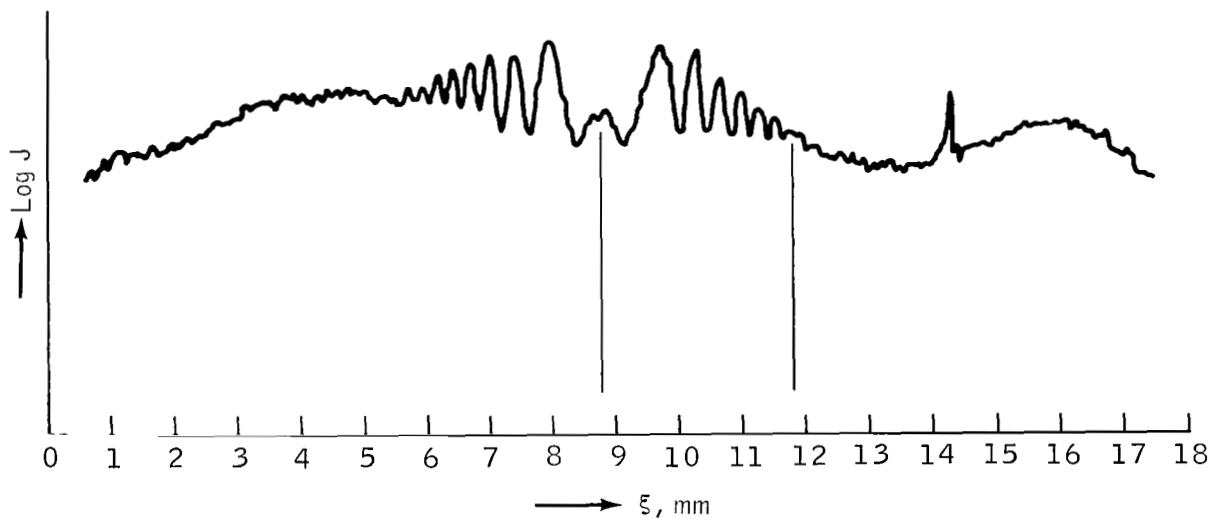

Figure 6. - Microdensitometer trace of experiment 2a.

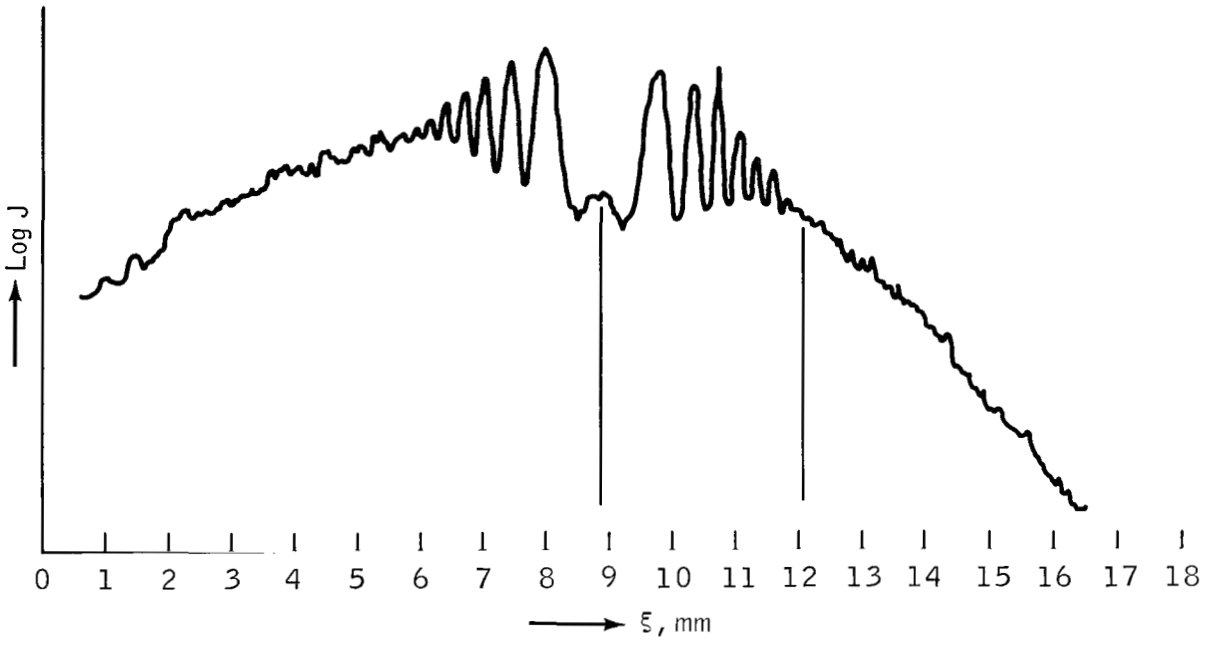

Figure 7. - Microdensitometer trace of experiment 2b.

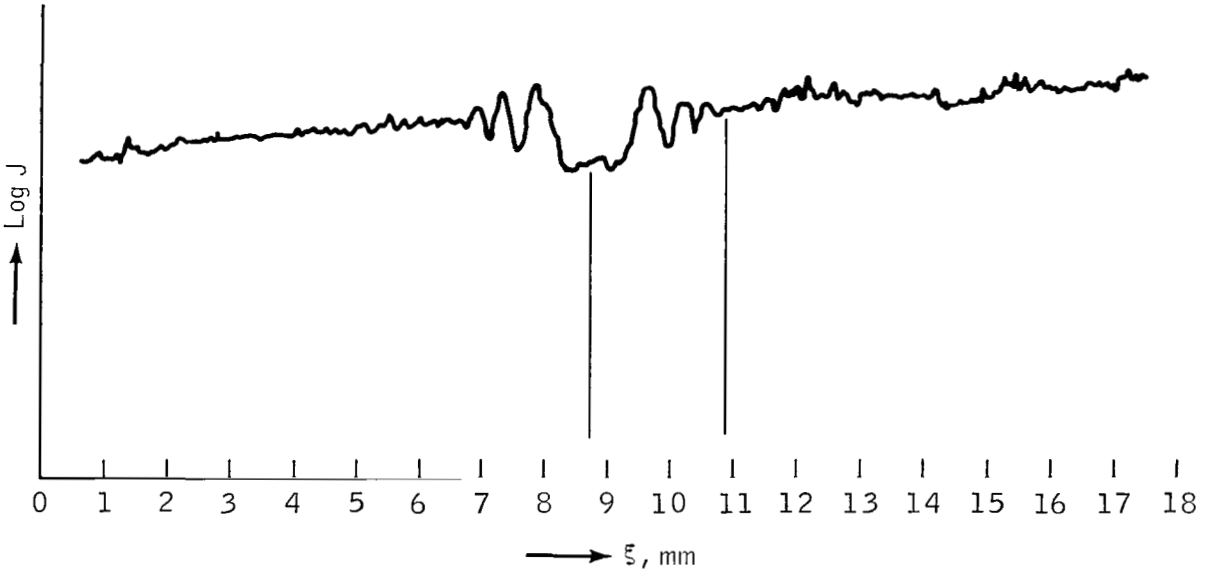

Figure 8. - Microdensitometer trace of experiment 3a.

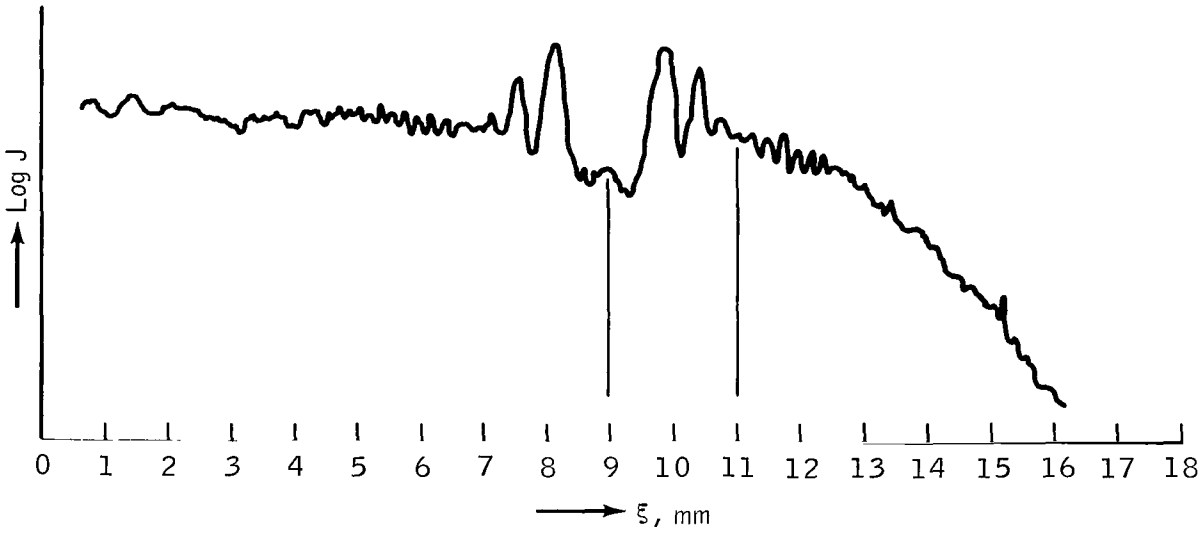

Figure 9. - Microdensitometer trace of experiment 3b.

TABLE II. - COMPARISON OF THEORETICAL AND EXPERIMENTAL RESULTS

Experiment no.	d, microns	$v\tau$, microns	Theoretical distance to first zero, mm	Measured distance to first zero, mm
1a	109	0	5.45	5.34
1b	109	0	5.45	5.75
2a	109	218	2.72	3.05
2b	109	218	2.72	3.20
3a	109	327	1.82	2.13
3b	109	327	1.82	2.05

Examination of table II shows that error exists in the experiment results. This error is explained on the basis of the following error sources.

1. Readings in revolutions per minute are related directly to velocity.

2. The linear actuator lead may have been in error. This error is related directly to velocity.

3. Location of the zeros on the microdensitometer traces was not precise.

4. The mechanical shutter on the camera was possibly inconsistent.

When all the possible error sources in the experiment are considered, the only error source that can affect the physical measurements of the diffraction pattern when the object is stationary is the location of the zeros on the microdensitometer traces. The conclusion is that the observed radical changes in the physical dimensions of the diffraction patterns are due solely to object motion. It is further concluded that a close correlation exists between the observed changes in physical dimensions and the changes predicted by this study. The purpose of this study was to establish the existence of the correlation; future studies can, no doubt, refine the technique used in this study.

CONCLUSIONS

This study has shown that it is possible to use the in-line Fraunhofer scheme to form a continuous-exposure hologram of an object in motion. The study has also given an expression for the recorded fringe pattern. This expression shows the effect of the object motion upon the usually recorded fringes which are proportional to the object geometry.

Manned Spacecraft Center
National Aeronautics and Space Administration
Houston, Texas, September 12, 1969
039-00-00-00-72

REFERENCES

1. DeVelis, J. B.; and Reynolds, G. O.: Theory and Applications of Holography. Addison-Wesley Publishing Co., 1967.

2. Parrent, G. B., Jr.; and Thompson, B. J.: Huygens' Principle. Society of Photo-Optical Instrumentation Engineers, vol. 3, Dec. 1964 and Jan. 1965, pp. 57-59.

3. Parrent, G. B., Jr.; and Thompson, B. J.: On the Fraunhofer (Far Field) Diffraction Patterns of Opaque and Transparent Objects With Coherent Background. Optica Acta, vol. 2, Apr. 1964, pp. 183-194.

4. Stroke, G. W.: An Introduction to Coherent Optics and Holography. Academic Press, 1966.

5. Thompson, B. J.: Diffraction by Opaque and Transparent Particles. Society of Photo-Optical Instrumentation Engineers, vol. 2, Dec. 1963 and Jan. 1964, pp. 53-56.

6. Powell, R. L.; and Stetson, K. A.: Interferometric Vibration Analysis by Wavefront Reconstruction. J. Opt. Soc. Am., vol. 55, Dec. 1965, pp. 1593-1598.

NASA-Langley, 1969 —— 14 S-220